PHYSICAL REVIEW B VOLUME 17, NUMBER 11 1 JUNE 1978

Crossover behavior of the magnetic phase boundary of the isotropic antiferromagnet $RbMnF_3$ from ultrasonic measurements

Y. Shapira and N. F. Oliveira, Jr.*

Francis Bitter National Magnet Laboratory, Massachusetts Institute of Technology, Cambridge, Massachusetts 02139

(Received 27 December 1977)

The ordering temperature $T_c(H)$ of the very nearly isotropic antiferromagnet $RbMnF_3$ was measured as a function of magnetic field H, up to 180 kOe. The order-disorder transition was determined from the λ peak in the attenuation of 26- to 82-MHz longitudinal waves. At all fields, T_c was measured with a precision of better than 2 mK. Results for the H dependence of T_c in two different samples (with Néel temperatures $T_N = 83.13 \pm 0.03$ K and 83.03 ± 0.03 K) were in very good agreement with each other. With increasing H, $T_c(H)$ first increases, then reaches a maximum, and finally decreases. The maximum in $T_c(H)$ is a mere 0.18 K above T_N. The phase boundary, T_c vs H, is bow-shaped and confirms the theoretical predictions of Fisher, Nelson, and Kosterlitz. Least-squares fits of the data for the two samples, supplemented by error analysis, give the values $\phi = 1.278 \pm 0.026$ and 1.274 ± 0.045 for the crossover exponent, in good agreement with the predicted value $\phi = 1.250 \pm 0.015$. The present data are in good agreement with, but are more precise than, the recent determination of the phase boundary of $RbMnF_3$ from thermal-expansion measurements. The experimental techniques employed to achieve high-precision thermometry in the presence of intense magnetic fields are discussed.

I. INTRODUCTION

Recent theoretical developments in the area of phase transitions and critical phenomena have stimulated an interest in crossover phenomena and multicritical points in magnetic systems.[1,2] Much of this interest has focused on the experimentally accessible multicritical points in antiferromagnets. Among the types of multicritical points found in antiferromagnets are the tricritical point in highly anisotropic antiferromagnets, and the bicritical point in weakly anisotropic antiferromagnets. The experimental studies (up to 1976) of these two types of multicritical points were reviewed by Wolf.[3] Several studies of bicritical points have been published since then.[4-7]

The present experimental work on the phase diagram of $RbMnF_3$ was stimulated by the striking predictions of Fisher, Nelson, and Kosterlitz (FNK) for the phase diagram of the completely isotropic three-dimensional Heisenberg antiferromagnet.[1,8] In mean-field theory (MFT), the ordering temperature $T_c(H)$ of such an antiferromagnet decreases with increasing magnetic field H; the decrease is proportional to H^2, at low H. In contrast, FNK have shown that as H is increased from zero, T_c first increases, passes through a maximum at some value of H, and only then decreases when H is increased still further (see Fig. 1). This behavior is the result of a crossover from a Heisenberg-like transition at $H = 0$ to an XY-like transition at finite H.

When a completely isotropic antiferromagnet becomes ordered at $H = 0$, all three components of the spin participate in the ordering process, i.e., the transition at the Néel temperature $T_N \equiv T_c(0)$ is Heisenberg-like. On the other hand, in the presence of a magnetic field $\vec{H}$, the staggered magnetization $\vec{L}$ in the ordered phase is forced to lie in the plane perpendicular to H. Therefore, for $H \neq 0$ the only spin components which become critical at $T_c(H)$ are the two spin components perpendicular to $\vec{H}$, i.e., the transition is XY-like. In MFT the number of critical spin components does not play a role in the determination of T_c (assuming a fixed magnitude for the exchange constant). On the other hand, calculations which include the effects of short-range order indicate that T_c tends to increase as the number of critical spin components decreases.[9] Therefore, in the case of the isotropic antiferromagnet, the H-induced change in the number of critical spin components (from 3 at $H = 0$, to 2 at finite H) leads to an initial increase of T_c with increasing H. This increase of T_c is counteracted by the usual depression (quadratic in H) of T_c by the magnetic field, which is predicted qualitatively by MFT. However, the quadratic term becomes dominant only above a certain finite value of H.

The detailed theory of FNK leads to the following H dependence of T_c for a completely isotropic antiferromagnet at low H:

$$T_c(H) - T_N = aH^{2/\phi} - bH^2, \tag{1}$$

where ϕ is the crossover exponent, and a and b are positive constants. The first term on the right-hand side of Eq. (1) represents the effect on

 © 1978 The American Physical Society

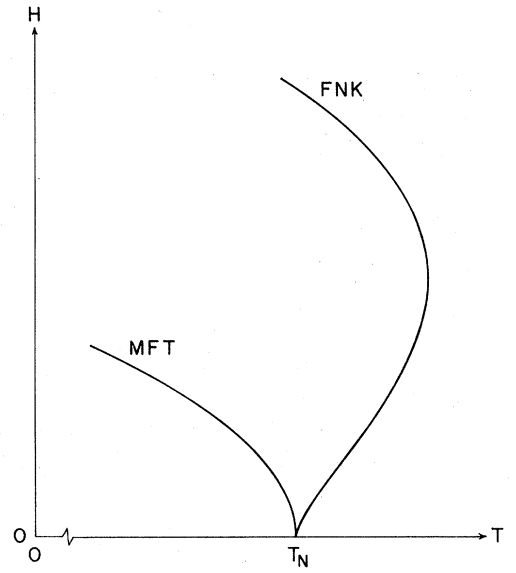

FIG. 1. Schematic of the T_c vs H phase boundary of a completely isotropic antiferromagnet near the Néel temperature T_N. The two curves represent the predictions of mean-field theory and of the Fisher-Nelson-Kosterlitz theory.

T_c of the crossover from a Heisenberg-like behavior at $H=0$ to an XY-like behavior at finite H. This term, by itself, would lead to an increase of T_c with increasing H. The second term is the leading nonlinear correction to scaling, and is analogous to the leading term in MFT. The net effect of both terms is that the boundary T_c vs H is bow-shaped, as shown in Fig. 1. The most reliable theoretical value for ϕ was obtained from high-temperature series expansions[10] which gave $\phi = 1.250 \pm 0.015$. It is noteworthy that Eq. (1) can be regarded as the zero-anisotropy limit of the expression for the "upper" phase boundary of a uniaxial antiferromagnet near the bicritical point.[1] Thus, the Néel point of a completely isotropic antiferromagnet may be regarded as a "degenerate bicritical point."[1]

$RbMnF_3$ is an excellent material for testing Eq. (1) and for obtaining an experimental value for the crossover exponent ϕ. It is a cubic antiferromagnet with one of the lowest ratios H_A/H_E between anisotropy and exchange fields ($H_A/H_E \cong 5\times10^{-6}$ for temperatures $T \ll T_N$). The Néel temperature $T_N = 83$ K lies in a fairly convenient experimental range, and the magnitude of the exchange field ($H_E \cong 800$ kOe at $T=0$) is not too high, so that a significant segment of the total phase diagram can be studied with presently available dc magnetic fields. Because of its many attractive features, $RbMnF_3$ has been studied by a variety of experimental techniques, and many of its magnetic properties are known.[11]

We consider briefly the deviation of $RbMnF_3$ from an ideal fully isotropic antiferromagnet. In the ordered phase of $RbMnF_3$, the small anisotropy causes the sublattice magnetizations at $H=0$ to lie along the $\langle 111\rangle$ directions. The equilibrium orientations of the sublattice magnetizations $\vec{M}_1$ and $\vec{M}_2$ (and that of the staggered magnetization $\vec{L}=\vec{M}_1-\vec{M}_2$) change when a magnetic field is applied. The H-induced reorientation of the sublattice magnetizations is discussed here only for the case when $\vec{H}$ is parallel to [100], which was the field orientation in the present experiments. As H is increased from zero, the sublattice magnetizations rotate until, at a field H_{sf}, they become very nearly perpendicular to $\vec{H}$. This process is analogous to the spin-flop transition in easy-axis antiferromagnets. However, because $\vec{H}$ is not parallel to any of the easy axes, the reorientation of the spins with increasing H (for $H \leq H_{sf}$) is gradual rather than abrupt. Theoretical analysis[12] and various experiments, including unpublished magnetostriction data taken by the present authors, indicate that at 4.2 K, the (pseudo-) spin-flop field H_{sf} is approximately 2.5 kOe. Our magnetostriction data also indicate that at 78 K, H_{sf} is between 1.0 and 1.5 kOe. The value of H_{sf} for T just below $T_N = 83$ K is expected to be approximately the same as at 78 K. The physical significance of H_{sf} is that for H well above H_{sf} the magnetic behavior is expected to approximate closely that of the ideal isotropic antiferromagnet. Because the present experiments were carried out in fields up to 180 kOe (i.e., $\sim 10^2 H_{sf}$), the effect of the anisotropy on the measured phase boundary T_c vs H was expected to be insignificant. The data for T_c vs H will be analyzed in terms of Eq. (1) for the ideal isotropic antiferromagnet. However, the possible effect of the anisotropy on the experimentally derived crossover exponent ϕ will be considered.

The first experimental test of Eq. (1) was carried out on $RbMnF_3$ recently.[13] In these earlier experiments, $T_c(H)$ was obtained from the λ anomaly in the thermal-expansion coefficient $\partial l/\partial T$, where l is the length of the sample. The thermal-expansion method is a fundamental method of determining T_c because $\partial l/\partial T$ is proportional to the second derivative of the thermodynamic potential $\Phi(T,H,P)$ with respect to T and the pressure P. The H dependence of T_c, in fields up to 180 kOe, obtained in these experiments was in good agreement with Eq. (1), and a least-squares fit of the data to this equation gave $\phi = 1.26$ for the crossover exponent, in good agreement with the theoretical value. The present experiments were undertaken with the objective of increasing the pre-

cision in the determination of the H dependence of T_c. To accomplish this objective, the experimental method of determining T_c was changed from thermal-expansion measurements to measurements of the ultrasonic attenuation. The advantage of the ultrasonic method is that the quantity which is being measured (namely, the attenuation) exhibits a λ anomaly. In contrast, in the thermal-expansion measurements, the length $l(H,T)$ at a fixed H is measured as a function of T, and the λ anomaly in $\partial l/\partial T$ is obtained only after the data are differentiated with respect to T. The direct observation of the λ anomaly with the ultrasonic method results in a higher precision, so that a more accurate value for the crossover exponent ϕ can be obtained. The results of both methods of determining T_c vs H are in very good agreement with each other. A preliminary report on the present work, as well as on results obtained in the isomorphic low-anisotropy antiferromagnet $KNiF_3$, was presented earlier.[14]

II. EXPERIMENTAL TECHNIQUES

A. Samples

The experiments were carried out on two $RbMnF_3$ single crystals. Both crystals were grown by the Crystal Physics Group, Center for Materials and Engineering, MIT. The first crystal (with $T_N = 83.13 \pm 0.03$ K) was the same one which was used earlier in the determination of $T_c(H)$ from thermal-expansion data.[13] The second crystal had a Néel temperature $T_N = 83.03 \pm 0.03$ K. (The quoted uncertainty for T_N represents the accuracy, rather than the precision.) These two crystals will be referred to as Nos. 1 and 2, respectively.

Each crystal was prepared with two parallel (100) faces separated by 7 mm. The ultrasonic measurements were performed with the ultrasonic pulse traveling back and forth between these two parallel faces. These parallel faces were also used for mounting the sample so that $\vec{H}$ was parallel to the [100] direction to within 2°.

B. Ultrasonic measurements

The attenuation of 26-to-82-MHz longitudinal ultrasonic waves propagating along [100] was measured. The ultrasonic waves were generated by X-cut quartz transducers bonded to the samples with Nonaq stopcock grease. Conventional pulse-echo techniques were used, and the attenuation was measured by gating the video signal from one of the echoes and measuring it with a boxcar integrator. The output of the integrator was fed to a digital voltmeter. A second digital voltmeter was used to read the thermometer (described below). The readings of both digital voltmeters were recorded simultaneously on a punch tape every 3 sec.

C. Magnetic fields and demagnetizing corrections

Magnetic fields were generated by two water-cooled Bitter-type solenoids. One of the solenoids produced a maximum field of 140 kOe, whereas the other produced fields up to 180 kOe. During each measurement of $T_c(H)$, the electrical current I through the solenoid (and hence H) was kept constant and the attenuation was measured as a function of T. The H vs I characteristic of the solenoid was calibrated at the end of each run with an accuracy of 0.25% using a Newport type-J integrator. The magnetic field was always parallel to the [100] crystallographic direction.

In experiments with magnetic materials one must distinguish between the external (applied) magnetic field H_{ext} and the internal field H_{int}. The two fields differ by the demagnetizing field H_d which depends on the shape of the sample. Because the significant field in these experiments is H_{int}, one must correct H_{ext} for the demagnetizing field. Using the known susceptibility of $RbMnF_3$ (Ref. 15) and the estimated demagnetizing factors for the two samples, it was estimated that $|H_d/H_{ext}| = 7\times10^{-4}$ for sample No. 1, and 9×10^{-4} for sample No. 2. Thus, the demagnetizing correction was quite small. All the results for the H dependence of T_c were corrected for the demagnetizing field.

D. Temperature control

The arrangement for controlling the temperature was the same as in Ref. 13. The sample was mounted on a copper block which was in a copper can filled with helium exchange gas. A second (outer) copper can surrounded the first (inner) can and was separated from it by a vacuum space. The outer can was surrounded by a liquid nitrogen bath ($T \cong 77$ K). A small heat leak caused the temperature of the sample to drift slowly toward the temperature of the nitrogen bath. For a sample temperature near $T_N = 83$ K the drift rate was ~10 mK/min. All final data were taken as T drifted down slowly in the presence of a fixed H.

E. Thermometry at high fields

The major experimental challenge in these measurements was the required high-precision thermometry in the presence of intense magnetic fields. To obtain meaningful data, the precision in the measurements of T had to be of the order of 1 mK at temperatures near 83 K, because the

maximum change in T_c caused by a field $H \leq 180$ kOe was a mere 0.18 K.

1. Thermometer

Temperatures were measured with a Keystone thermistor resistance thermometer,[16] similar to the one used in Ref. 13. However, whereas the thermistor used in the earlier work was embedded in the copper block on which the sample rested, in the present work the thermistor was attached directly to the sample with G.E. 7031 varnish. The copper leads to the thermistor were also anchored thermally to the sample. This arrangement minimized the temperature gradient between the sample and the thermometer. Checks made by comparing data taken in increasing temperatures (produced by a heater wound on the outer surface of the inner can) with those for decreasing temperatures (with the heater turned off) showed no hysteresis in $T_c(H)$ greater than the experimental resolution of ~2 mK.

The temperature characteristic of the thermistor thermometer was calibrated *in situ*, at $H = 0$, against a platinum resistance thermometer mounted on the copper block inside the inner can. The data for this calibration were taken between 77 and 85 K. Over this temperature range, $\log R$ was approximately linear in T, where R is the resistance of the thermistor. Since this linearity was only approximate, a calibration curve (R vs T) was obtained by fitting $\log R$ to a second-degree polynomial in T. The slope $d(\log R)/dT$ near T_N, obtained from this fit, was accurate to better than 1%. The advantages of using the thermistor as a thermometer were: a higher sensitivity $[(1/R)(\partial R/\partial T) = -3.7\%/\mathrm{K}]$ and a much smaller magnetoresistance than those for the platinum thermometer. The high sensitivity allowed T to be measured with a precision of ~1 mK.

The measurements of T_c vs H in sample No. 1 were performed over a period of one week, whereas those in sample No. 2 took place over a period of nearly three weeks. Between experimental runs with the same sample, the sample holder was kept immersed in liquid nitrogen. Thus, during the course of measurements with either sample, the temperature of the sample (and, hence, of the thermistor thermometer) was maintained between 77 and 85 K. Calibrations of the thermistor thermometer against the platinum thermometer were performed during the measurements on either of the two samples. Repeated measurements of the ordering temperature T_c at $H = 0$ in sample No. 1 showed that the calibration of the thermistor thermometer did not change by more than 2 mK during the course of measurements with this sample.

Similar checks of the reproducibility of the thermistor thermometer were also performed during the measurements on sample No. 2, but in this case the reproducibility of the transition at $H = 1$ kOe rather than at $H = 0$ was monitored (see Sec. III B). These checks also showed that the thermistor was reproducible to within 2 mK.

The reproducibility of the thermistor thermometer was also monitored over a period of several months, during which time the thermistor was cycled many times from room temperature to liquid-nitrogen temperature. Some of these temperature cycles involved direct immersion in liquid nitrogen. Although many temperature cycles did not have an appreciable effect on the calibration of the thermistor thermometer, some temperature cycles changed the calibration of the thermistor by ~1 K. The temperature cycles did not change the sensitivity of the thermistor thermometer, $(1/R)(dR/dT)$, by more than 3% during the entire period of several months.

The measurements of the H dependence of T_c in any experimental run included the following steps: The transition temperature at $H = 0$ was measured several times during the run. All values for $T_c(H)$ obtained during the run were then determined relative to the zero-field transition temperature measured in the same run. In the experiments with sample No. 2, it was sometimes advantageous to measure $T_c(H)$ relative to $T_c(H = 1\ \mathrm{kOe})$ instead of $T_c(H = 0)$. (See Sec. III B).

2. Magnetoresistance of thermometer

Temperature measurements in a magnetic field require a correction for the effect of H on the thermometer. The thermistor used in the present experiments was nominally the same as the original thermistor used in the earlier thermal-expansion work,[13] and had very similar characteristics. Extensive measurements of the isothermal magnetoresistance $\Delta R = R(H) - R(0)$ of the original thermistor were made using two different methods. In the first method, the temperature of the inner can was stabilized near $T_N = 83$ K and ΔR was measured by changing H from zero to a given value and then back to zero. In the second method, the magnetoresistance was measured at 77 and 87 K, with the thermistor immersed in short columns of boiling liquid nitrogen and liquid argon, respectively. The magnetoresistance at the operating temperature 83 K was calculated by interpolating between the results for $\Delta R(H)$ at 77 and 87 K. The results of both methods agreed with each other.

Several experimental checks were made and several precautions were taken in connection with the above two methods of determining ΔR. Concerning

the first method, we examined the possibility of a magnetocaloric effect, i.e., an H-induced change in the temperature of the sample (which would lead to a small temperature change of the entire assembly inside the inner can). To check this possibility, the measurements were repeated with the $RbMnF_3$ sample removed from the inner can. The results with and without the sample, in fields up to 180 kOe, were the same to within ~3 mK. Another check of the first method was designed to simulate the usual temperature difference between the operating temperature 83 K and the liquid bath's temperature 77 K. To this end, the temperature of the liquid bath was reduced to 72 K by pumping on the liquid nitrogen, and the magnetoresistance was measured at 77 K. Subsequently, the magnetoresistance at 77 K was measured by the second method, i.e., by immersing the thermistor in a short column of liquid nitrogen. The two determinations of $\Delta R(H)$ at 77 K agreed with each other.

The main precaution with the second method was the necessity of keeping the column of the boiling liquid short, in order to minimize the variation of the magnetic field along the column. This precaution was necessary because the magnetic force on a column of a boiling liquid which extends from the center of the magnet to well outside the magnet can change the temperature of the liquid at the center of magnet. For a diamagnetic liquid the magnetic force lowers the hydrostatic pressure head, whereas for a paramagnetic liquid the effect is opposite. Calculations and experiments[17] indicate that even for the small susceptibilities of liquid nitrogen and liquid argon, temperature changes of order 10 mK can occur in fields of ~100 kOe. By keeping the liquid column short (i.e., confined to a region in which H changed only slightly) the expected temperature change at the highest field was kept below 1 mK.

The earlier measurements of ΔR, performed in connection with the work in Ref. 13, showed that at 77, 83, and 87 K, ΔR was proportional to H^2. At 83 K the magnetoresistance at 180 kOe was equivalent to $-(40 \pm 9)$ mK.

The magnetoresistance of the thermistor used in the present work was measured at 83 K by the first method, with the $RbMnF_3$ sample in the inner can. The results showed that the magnetoresistance at 180 kOe was equivalent to $-(42 \pm 4)$ mK. Measurements at 77 and 87 K using the second method (i.e., direct immersion in a short column of a boiling liquid) showed that the magnetoresistance was proportional to H^2 at both temperatures. By interpolation, the magnetoresistance near 83 K for $H = 180$ kOe was equivalent to $-(42 \pm 6)$ mK, where the uncertainty represents the difference between values obtained with different "reasonable" interpolation procedures. All temperatures measured in the present work were corrected for a magnetoresistance ΔR proportional to H^2, with a proportionality constant equivalent to -42 mK at 180 kOe.

3. *Uncertainty in the magnetoresistance*

The uncertainty in ΔR leads to an uncertainty in the experimentally determined values of $T_c(H)$. The significance of this source of experimental uncertainty is now considered.

For all values of H, the *total* magnetoresistance ΔR, expressed as a change in T, was always smaller than $0.3\,[T_c(H) - T_c(0)]$. The *uncertainty* in the magnetoresistance was smaller than $0.04[T_c(H) - T_c(0)]$. Thus, the uncertainty in the magnetoresistance corresponds to a relatively small uncertainty in the observed phase boundary.

Because ΔR is proportional to H^2, the uncertainty in the proportionality constant implies that all the experimental values of $T_c(H)$ may differ from the true values by a term which is proportional to H^2. We now note that Eq. (1) contains a term proportional to H^2, namely, $-bH^2$. It can be shown that when the data for $T_c(H)$ are fitted to Eq. (1), any systematic error in the values of $T_c(H)$ which is proportional to H^2 will merely change the experimentally determined coefficient b which appears in this equation. Thus, the uncertainty in ΔR leads to an uncertainty in the experimental value of b. As shown later, $bH^2 \cong 1300$ mK at 180 kOe, so that a 6-mK uncertainty in ΔR at 180 kOe would lead to an uncertainty of 0.5% in the value of b. It is significant that an error in the proportionality constant between ΔR and H^2 will affect only the parameter b, but the parameters a and ϕ determined from a fit of the data to Eq. (1) will not be affected. Thus, the experimentally determined crossover exponent ϕ is not affected by the uncertainty in the magnetoresistance.

III. ATTENUATION PEAKS

Because the H dependence of T_c was determined from peaks in the attenuation of longitudinal ultrasonic waves, some features of these peaks and the manner of obtaining $T_c(H)$ will be described. The measurements in sample No. 1 were performed with a 45-MHz ultrasonic wave, whereas those in sample No. 2 were performed with 26- and 82-MHz waves. The attenuation was measured as a function of T at a fixed H. Typical results are shown in Fig. 2. The two attenuation peaks in this figure are associated with the order-disorder transitions at two magnetic fields. Note that the attenuation peak for the higher field is larger. Other data show a monotonic increases with in-

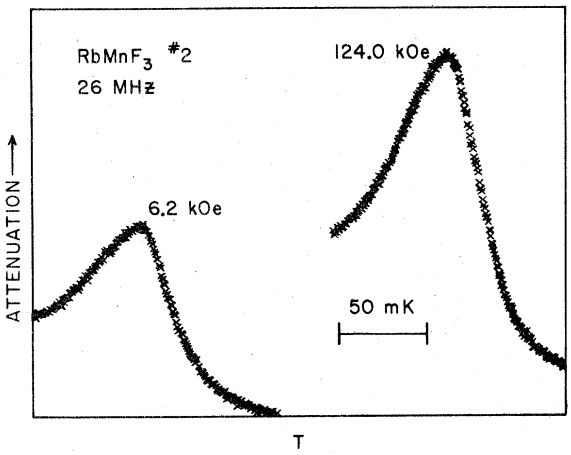

FIG. 2. Temperature dependence of the attenuation of a 26-MHz longitudinal ultrasonic wave in $RbMnF_3$ (sample No. 2) at $H = 6.2$ and 124.0 kOe. Both the direction of sound propagation and the direction of $\vec{H}$ are parallel to the [100] axis.

creasing H of the height of the attenuation peak. For the data in Fig. 2, the transition at the higher field occurs at a higher temperature.

To illustrate the precision in the determination of the temperature T_{max} at the attenuation maximum, we present in Fig. 3 detailed results at $H = 0$ for sample No. 1. The horizontal spacings between the points in Fig. 3 are integer multiples of 0.6 mK. The estimated precision in the determination of T_{max}, in both samples and for all H, was better than 2 mK. This estimate is consistent with both the rms deviations and the maximum deviations between the experimental points for

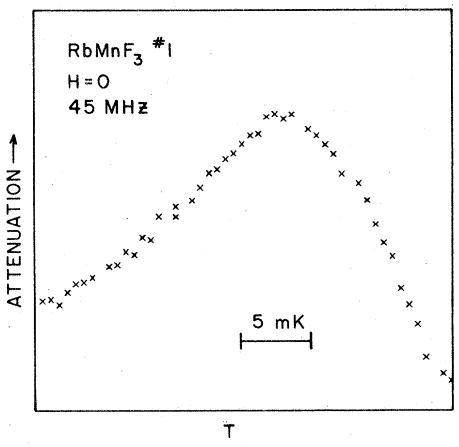

FIG. 3. Temperature dependence of the attenuation of a 45-MHz longitudinal ultrasonic wave in $RbMnF_3$ (sample No. 1) at $H = 0$. The direction of sound propagation is parallel to [100]. Only the data near the attenuation peak (i.e., near T_N) are shown here.

$T_c(H)$ and the best fits of these data points to Eq. (1) (see Sec. IV).

A. Method of determining the H dependence of T_c

Previous studies at $H = 0$ have shown that in $RbMnF_3$ (and in some other antiferromagnets) the temperature T_{max} at the maximum of the attenuation peak depends very slightly on the ultrasonic frequency.[18,19] The Néel temperature in these studies was identified as the zero-frequency limit of T_{max}. Because the present experiments were performed at finite frequencies, there arises the question of the distortion, if any, in the values of $T_c(H) - T_c(0)$ determined from the H dependence of T_{max} for a finite frequency. Several observations are relevant to this question: (i) According to Moran and Lüthi,[18] T_{max} for a 70-MHz wave in $RbMNF_3$ differs from T_N by less than 5 mK. (ii) Comparison between $T_{max}(H = 0)$ for a 45-MHz wave in (our) sample No. 1 and the maximum of the thermal expansion in the same sample indicates that the two temperatures do not differ by more than 10 mK. (Both of these measurements were made using the platinum resistance thermometer. The uncertainty of 10 mK represents the precision of these experiments.) Since the validity of the determination of T_N from the peak in the thermal expansion is justified by thermodynamics, the difference between T_{max} for the 45-MHz wave and T_N is less than 10 mK. This is consistent with the observation of Moran and Lüthi. (iii) The important question which remains is whether the H dependence of T_{max} depends on frequency. If it does, then $T_{max}(H) - T_{max}(0)$ cannot be taken as $T_c(H) - T_c(0)$. To answer this question, the experiments in sample No. 2 were carried out using two different frequencies. Although the most detailed and most precise data were obtained at 26 MHz, extensive data on the same sample were also taken at 82 MHz in fields up to 140 kOe. For any fixed H, the values for T_{max} for these two frequencies did not differ by more than the combined experimental uncertainty of 4 mK. Moreover, fits of the 82-MHz data to Eq. (1) led to results which were in good agreement with those obtained from similar fits for the 26-MHz data. On this basis we conclude that the use of finite frequency in the present experiments had a negligible effect on the determination of $T_c(H) - T_c(0)$. The last conclusion is reinforced by the very good agreement between the ultrasonic and thermal-expansion data for T_c vs H in sample No. 1.

B. Attenuation at low H

In fields above ~1 kOe, the attenuation for $T < T_{max}$ decreases monotonically with decreasing T.

This is illustrated by the data in Fig. 2, but is also true for a wider temperature range than that shown in this figure. Thus, the attenuation above ~1 kOe exhibits a "simple" λ peak. The situation for fields below ~1 kOe is more complicated. This is illustrated in Fig. 4 which shows the T dependence of the zero-field attenuation for a 45-MHz wave in sample No. 1. The data in Fig. 4 were obtained in the same run as those in Fig. 3, but cover a much wider temperature interval. In this case, the attenuation below T_N does not decrease monotonically with decreasing T. Instead, as T decreases below T_N, the attenuation first decreases, then passes through a minimum, and then increases. The latter increase indicates the existence of another attenuation mechanism (or mechanisms) below T_N. Several possible attenuation mechanisms which may exist below T_N are discussed in Ref. 18. Among these, we consider the magnetoelastic coupling described by Melcher and Bolef[20] as a likely possibility. When the ultrasonic-propagation direction and $\vec{H}$ are both parallel to [100], the attenuation due to the magnetoelastic coupling is expected to disappear when H exceeds the (pseudo-) spin-flop field H_{sf}, i.e., when the sublattice magnetizations become perpendicular to $\vec{H}$. Experimentally, the additional attenuation below T_N disappears when H exceeds ~1 kOe, which is approximately the value of H_{sf} for temperatures just below T_N.

The additional attenuation below T_c, for $H < 1$ kOe, made the precise determination of $T_c(H)$ at these fields more difficult, because this additional attenuation shifted the maximum in the (total) attenuation from where it would have been otherwise. For the example in Fig. 4, the estimated shift was a mere 0.2 mK. The shift in the attenuation maximum for the 82-MHz wave in sample No. 2 was also very small. However, for the 26-MHz wave in sample No. 2, the additional attenuation below T_N was large compared to the critical attenuation peak at T_N, and it was not possible to determine the zero-field transition accurately. For this reason, all the 26-MHz data for $T_c(H)$ in sample No. 2 were obtained in fields $H \geq 1$ kOe.

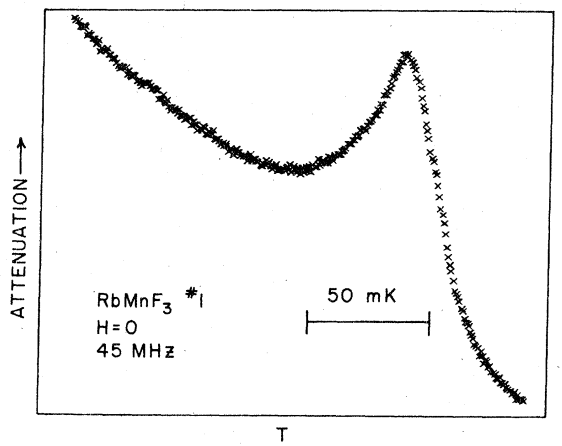

FIG. 4. Zero-field attenuation vs T in sample No. 1. These data are for the same experimental run as in Fig. 3, but cover a much wider temperature range.

Because of the complications which existed below 1 kOe, the following procedures were used to fit the data for $T_c(H)$ to Eq. (1): The 45-MHz data for $T_c(H)$ in sample No. 1 were first fitted to Eq. (1) with T_N held fixed at its experimentally determined value. Subsequently, the data point at $H = 0$ (i.e., for T_N) was ignored, and a fit to Eq. (1) was made by treating T_N as an adjustable parameter. The results of both fits were very close to each other. In particular, the crossover exponents obtained from the two fits differed by only 0.014. The numerical values quoted in Secs. IV and V for sample No. 1 are those obtained from the first fit (with fixed T_N), but the estimate of the uncertainty in ϕ takes into consideration the results of the second fit. All fits to the 26-MHz data for sample No. 2 were made by treating T_N as an adjustable parameter, because a sufficiently precise value for T_N was not available in this case. The lowest-field datum point for these fits was at $H = 1$ kOe. The values of T_N in sample No. 2 obtained from various fits had standard deviations of 0.4 mK or less, and all agreed with each other to within 0.6 mK. All data for sample No. 2 are plotted relative to the value of T_N obtained by fitting all the data between 1.0 and 178.5 kOe to Eq. (1), with T_N, a, b, and ϕ treated as adjustable parameters.

IV. H DEPENDENCE OF T_c

A. Experimental results

The H dependence of T_c for sample No. 1 is shown in Fig. 5. These data were obtained from the attenuation maxima for a 45-MHz wave. The H dependence of T_c in sample No. 2, obtained from the attenuation peaks for a 26-MHz wave, are shown in Fig. 6. Note that the total temperature interval in Figs. 5 and 6 is $2\times10^{-3}T_N$. Comparison of these two figures indicates that the results for $T_c(H) - T_N$ in both samples are in very good agreement with each other. These results are also in very good agreement with the earlier determination of this phase boundary from thermal-expansion measurements.[13]

The phase boundary in either Fig. 5 or 6 is a bow-shaped curve, with a T_c which increases with increasing H at low H. These distinctive features confirm the predictions of the FNK theory. The

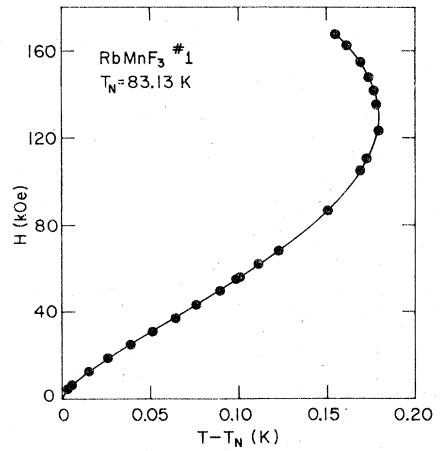

FIG. 5. H dependence of the order-disorder transition temperature $T_c(H)$ in sample No. 1. The solid curve is a least-squares fit of these data to Eq. (1), with a, b, and ϕ treated as adjustable parameters (see text).

solid curves in Figs. 5 and 6 are least-squares fits of the data to Eq. (1), with a, b, and ϕ treated as adjustable parameters. (As noted earlier, for sample No. 2, T_N is also adjustable.) The least-squares fits will be discussed later.

The curvature of the phase boundary, in either Fig. 5 or 6, changes sign. Starting at the origin and moving along the phase boundary, the concave side of the curve is first on the right-hand side (negative curvature), and then on the left-hand side (positive curvature). This feature is expected from Eq. (1) and the theoretical value of ϕ. Equation (1) also predicts that the phase boundary in the T-H plane is vertical at $T=T_N$, $H=0$. Figure 7 shows the detailed variation of the phase boundary at low H. The total temperature interval in this figure is $5\times10^{-4}\ T_N$. Note that (i) the results for both samples are in close agreement; (ii) the theoretical prediction concerning the curvature of the phase boundary at low H is confirmed; (iii) the phase boundary appears to be vertical at the origin; and (iv) the solid curve which is a fit to Eq. (1) of *all* the data for sample No. 1 (up to 168 kOe) describes the low-H data quite well. [The low-H portion of the fit of all the data for sample No. 2 (up to 178.5 kOe) is practically identical to the solid curve in Fig. 7, differing from it by less than 0.4 mK.]

B. Least-squares fits

Two types of least-squares fits were performed. In the first, the data were fitted to Eq. (1) treating ϕ as well as a and b as adjustable parameters. In the second, a and b were allowed to vary, but ϕ was kept fixed at its theoretically predicted value of 1.250.

The parameters obtained from the first type of fit to the data in Figs. 5 and 6 (separately) are listed in Table I. Also included in Table I are the results of a fit of the $T_c(H)$ data in Ref. 13, which were obtained from thermal-expansion measurements in sample No. 1. The rms deviation δT between the measured values of $T_c(H)$ and those calculated from the fit is also listed in Table I. For the data in Fig. 5, $\delta T=0.50$ mK, and the maximum deviation between any measured T_c and the fit is 1.0 mK. For the data in Fig. 6, $\delta T=0.71$ mK, and the maximum deviation is 1.6

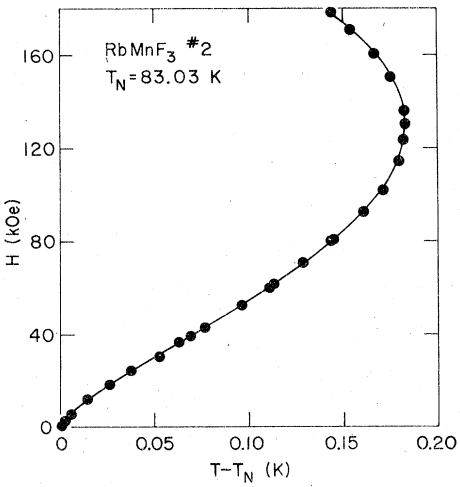

FIG. 6. H dependence of the order-disorder transition temperature $T_c(H)$ in sample No. 2. The solid curve is a least-squares fit of these data to Eq. (1), with a, b, ϕ, and T_N treated as adjustable parameters (see text).

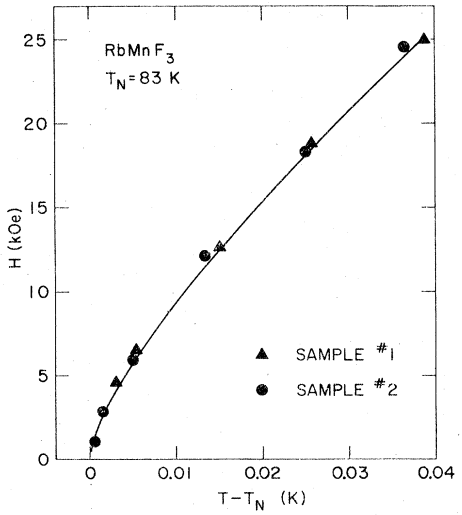

FIG. 7. H dependence of T_c for fields $H<25$ kOe. Results for both samples are shown. The solid curve is the low-H portion of the least-squares fit shown in Fig. 5.

TABLE I. Results of least-squares fits of the data to Eq. (1), with ϕ, a, and b treated as adjustable parameters. For these fits, H is in units of 10^4 Oe, and T is in units of degrees K. σ_ϕ is the standard deviation for ϕ (see Sec. V A). δT is the rms deviation (in units of degrees K) between the measured $T_c(H)$ and the best fit.

Sample No.	Method	a	b	ϕ	σ_ϕ	δT	Reference
1	Thermal expansion	1.4614×10^{-2}	4.0439×10^{-3}	1.2577	0.014	1.47×10^{-3}	13
1	Ultrasonic 45 MHz	1.4793×10^{-2}	3.7804×10^{-3}	1.2784	0.006	0.50×10^{-3}	This work
2	Ultrasonic 26 MHz	1.5002×10^{-2}	3.8944×10^{-3}	1.2741	0.010	0.71×10^{-3}	This work

mK. These values are consistent with the estimated precision of 2 mK for the values of T_c obtained in the present work. Note that for the data in Ref. 13, $\delta T = 1.47$ mK, which is considerably larger than for the present data.

The results for the second type of fit, with ϕ held fixed at 1.250, are listed in Table II.

Tables I and II show that the coefficient b is approximately equal to 4×10^{-11} K/Oe^2. As shown in Ref. 13, this value is comparable to the proportionality constant between $T_c(H) - T_N$ and H^2 obtained from MFT. This is not surprising because the term $-bH^2$ in Eq. (1) is analogous to the leading term in MFT.

An attempt for a more quantitative comparison between the experimental value of b and theory was made by considering the isotropic antiferromagnet as a uniaxial antiferromagnet with arbitrarily small anisotropy. The idea was to relate the parameter b in the isotropic case to some parameter in the more extensively studied anisotropic case. The starting point for the estimate of b was Fisher's observation[1] that Eq. (1) can be regarded as the zero-anisotropy limit of the equation for the "upper" phase boundary near the bicritical point of a uniaxial antiferromagnet, i.e., the boundary $T_c^{\perp}(H^2)$ separating the spin-flop phase from the paramagnetic phase. The discussion of Eq. (6) of the present paper then suggests that $b = qT_N$, where q is a parameter which appears in Eq. (5) and is related to one of the scaling axes near the bicritical point. Fisher[1] has given an estimate for q in terms of the mean-field slope of the "lower" phase boundary for a uniaxial antiferromagnet, i.e., the boundary $T_c^{\parallel}(H^2)$ separating the antiferromagnetic phase from the paramagnetic phase when $\vec{H}$ is parallel to the easy axis. His estimate for the case of a uniaxial antiferromagnet is

$$q = -(5/9T_N)[dT_c^{\parallel}/d(H^2)], \tag{2}$$

where we have replaced the bicritical temperature T_b by T_N, and have set n (the number of critical spin components at the multicritical point) equal to 3. The parameter b for $RbMnF_3$ was calculated from Eq. (2) and the suggested relation $b = qT_N$. The mean-field expression[21] for the slope $[dT_c^{\parallel}/d(H^2)]$ in terms of the exchange constant J, and the value[15,22] $J = -3.4$ K, were used. The estimated value of b obtained in this fashion was 4×10^{-11} K/Oe^2, in very good agreement with experiment (see Ref. 23).

Equation (1) may also be rewritten in terms of the reduced field $H/2H_E(0)$ and the reduced tem-

TABLE II. Results of least-squares fits of the data to Eq. (1), with ϕ held fixed at its theoretical value of 1.250, and with a and b treated as adjustable parameters. For these fits, H is in units of 10^4 Oe, and T is in units of degrees K. δT is the rms deviation (in units of degrees K) between the measured $T_c(H)$ and the best fit.

Sample No.	Method	a	b	δT	Reference
1	Thermal expansion	1.4615×10^{-2}	4.1731×10^{-3}	1.48×10^{-3}	13
1	Ultrasonic 45 MHz	1.4834×10^{-2}	4.2531×10^{-3}	0.72×10^{-3}	This work
2	Ultrasonic 26 MHz	1.4923×10^{-2}	4.2689×10^{-3}	0.79×10^{-3}	This work

perature T/T_N, where $H_E(0)$ is the exchange field at $T=0$. This alternative was discussed in Ref. 13 and the values $H_E(0)=890$ kOe and $T_N=83.13$ K were used. However, we have since recognized that more reliable values[15,22] for $H_E(0)$ in $RbMnF_3$ are lower than 890 kOe by 15%. The alternative (reduced) form of Eq. (1) will not be considered here.

V. CROSSOVER EXPONENT

The values for the crossover exponent ϕ derived from the fits of the experimental data in Figs. 5 and 6 to Eq. (1) are listed in Table I. To evaluate the uncertainties in these values, several sources of errors were considered.

A. Random errors

Consider first the uncertainty caused by random experimental errors in the determination of $T_c(H)$, which are a consequence of the finite experimental precision. The analysis of these errors was similar to that described by Bevington.[24] The errors in the experimental points for $T_c(H)$ were considered to be independent of each other. These errors were assumed to follow a single normal distribution with a variance σ_T^2. The latter variance was estimated from the rms deviation δT between the measured values of $T_c(H)$ and those calculated from the least-squares fit, namely,

$$\sigma_T^2=[N/(N-\nu)](\delta T)^2, \tag{3}$$

where N is the number of data points and ν is the number of adjustable parameters in the fit. Because the crossover exponent ϕ derived from a fit is a function of the measured values $T_c(H)_i$ used in the fit ($i=1,2,\ldots,N$), the standard deviation σ_ϕ for ϕ is given by

$$\sigma_\phi^2=\sum_i \sigma_T^2\left(\frac{\partial\phi}{\partial T_c(H)_i}\right)^2. \tag{4}$$

The partial derivatives in Eq. (4) were determined as follows: A least-squares fit was first performed to all the data points $T_c(H)_i$. Subsequently, one of the data points, say $T_c(H)_j$, was changed by a small amount Δ while all other data points remained unchanged. A least-squares fit to the modified set of points was then performed and yielded a new value for ϕ. The derivative of ϕ with respect to $T_c(H)_j$ was then calculated from the change in ϕ caused by the (small) change in $T_c(H)_j$. This calculated derivative was found to be very nearly independent of Δ for $\Delta \lesssim \sigma_T$. By changing the data points $T_c(H)_i$ by Δ (one at a time, and leaving all other points at their original values) and performing the corresponding least-squares fits, all the derivatives in Eq. (4) were evaluated. The standard deviations for ϕ calculated from Eq. (4) in this fashion are listed in Table I.

Apart from the analysis of the random errors, the following questions were considered: How consistent are the data obtained in different experimental runs? What would be the effect of treating T_N as an adjustable parameter? (This question is relevant only to the data for sample No. 1, because in the fits for the second sample T_N was already treated as an adjustable parameter.) What is the effect on ϕ of the small anisotropy in $RbMnF_3$? Does the experimentally derived value of ϕ depend on the range of applied fields?

B. Consistency checks

The data for each of the two samples were obtained in two separate experimental runs, carried out with two different magnets. A measure of the consistency in the determination of ϕ was obtained by comparing the results of least-squares fits to data obtained in the separate runs. The two values of ϕ for sample No. 1 were 1.272 and 1.288, i.e., within 0.010 from the value in Table I. For sample No. 2, the values of ϕ were 1.249 and 1.291, i.e., within 0.025 from the value in Table I.

A new fit to the data for sample No. 1 was performed by regarding T_N (in addition to ϕ, a, and b) as an adjustable parameter. This may be justified by the fact that the experimental value for T_N is also subject to error, and the error in T_N may be larger than for other data points (see Sec. III). Owing to this consideration, the data point for T_N was not included in the fit with the adjustable T_N. This fit gave a value for ϕ which was 0.014 larger than that in Table I, and an (adjusted) Néel temperature which was 0.76 mK lower than the best experimental value.

C. Possible effect of anisotropy

An attempt was also made to estimate the effect of the small anisotropy in $RbMnF_3$ on the experimentally derived ϕ. The effect of anisotropy on the phase boundaries of a *uniaxial* antiferromagnet has been studied both theoretically[1,8] and experimentally.[3-7] In the uniaxial case the most pronounced effect of the anisotropy on the phase boundary is realized when $\vec{H}$ is parallel to the easy axis. $RbMnF_3$ is a cubic antiferromagnet with easy axes along the $\langle 111\rangle$ directions, and is, therefore, not a uniaxial antiferromagnet. Nevertheless, it was felt that an upper limit for the effect of the anisotropy on the experimentally derived ϕ could be obtained by considering

$RbMnF_3$ to be a uniaxial antiferromagnet with $\vec{H}$ parallel to the easy axis. The bicritical field H_b of this fictitious uniaxial antiferromagnet was set equal to the (pseudo-) spin-flop field H_{sf} in $RbMnF_3$. As noted in Sec. I, for $\vec{H}$ parallel to [100] and for T just below T_N, $H_{sf} \lesssim 1.5$ kOe.

The phase boundary of a uniaxial antiferromagnet when $\vec{H}$ is parallel to the easy axis and for fields just above H_b is given by

$$H^2 - H_b^2 - pt = w_\perp [t + q(H^2 - H_b^2)]^\phi , \qquad (5)$$

where $t = (T_c - T_b)/T_b$ is the reduced temperature at the transition, T_b is the temperature at the bicritical point, p is a constant related to the temperature derivative of the spin-flop field, and q and $w_\perp$ are constants (see Ref. 1). Equation (1) can be regarded as the limit of Eq. (5) when the anisotropy tends to zero. For $RbMnF_3$ the parameter p is very small and can be set equal to zero. Equation (5) then gives

$$T_c - T_b = a^* h^{2/\phi} - b^* h^2 , \qquad (6)$$

where $h = (H^2 - H_b^2)^{1/2}$, $a^* = T_b w_\perp^{-1/\phi}$, $b^* = qT_b$. Equation (6) is the same as Eq. (1), with T_N replaced by T_b and with H replaced by $h = (H^2 - H_b^2)^{1/2}$. The data for sample Nos. 1 and 2 were fitted to Eq. (6). In these fits, T_b was treated as an adjustable parameter, H_b was set equal to 1.5 kOe, and all data points for $H < 1.5$ kOe were deleted. These fits gave $\phi = 1.290$ for sample No. 1, and $\phi = 1.274$ for sample No. 2.

D. Final values of ϕ

Apart from the uncertainty due to random experimental errors, the various checks described above lead to values for ϕ which do not differ from those in Table I by more than $(\Delta\phi)_{max} = 0.014$ for sample No. 1, and $(\Delta\phi)_{max} = 0.025$ for sample No. 2. Our final estimate for the uncertainty in ϕ was chosen to be equal to $(\Delta\phi)_{max} + 2\sigma_\phi$. Thus our final values for ϕ are 1.278 ± 0.026 for sample No. 1, and 1.274 ± 0.045 for sample No. 2.

The recent study[13] of the phase boundary in sample No. 1 from thermal-expansion measurements gave $\phi = 1.258$, but an error analysis was not performed at that time. A new analysis of the same data gives $\sigma_\phi = 0.014$, and an estimated uncertainty of ± 0.08. These results are summarized in Table III. It is apparent that the experimental values for the crossover exponent

TABLE III. Results for the crossover exponent ϕ.

Sample No.	Method	ϕ	Reference
1	Thermal expansion	1.258 ± 0.08	13
1	Ultrasonic 45 MHz	1.278 ± 0.026	This work
2	Ultrasonic 26 MHz	1.274 ± 0.045	This work
...	Theory	1.250 ± 0.015	10

in $RbMnF_3$ are in agreement with the theoretical value $\phi = 1.250 \pm 0.015$.

E. Dependence of ϕ on the range of H

The above analysis implicitly assumed that Eq. (1) holds over the entire range of magnetic fields used in the present experiments. As a check, the dependence of the experimentally derived ϕ on the range of H used in the fit to Eq. (1) was examined. Least-squares fits which were restricted to data points with H below some chosen value H_{max} were performed. The omission of high-field data points led to a larger standard deviation σ_ϕ, i.e., σ_ϕ increased as the number of data points included in the fit decreased. Thus, meaningful values for ϕ could not be obtained for arbitrarily low H_{max}. The results of such fits for both samples indicated that for all fields H_{max} above 80 kOe the experimentally derived ϕ was within the uncertainties listed in Table III. For $H_{max} \lesssim 80$ kOe the standard deviation σ_ϕ for either sample exceeded the total uncertainty listed in Table III, and was considered too large for drawing a meaningful conclusion. The results for $H_{max} > 80$ kOe indicate that the use of Eq. (1) to fit data up to 180 kOe was reasonable.

In conclusion, both the qualitative shape of the boundary $T_c(H)$ for $RbMnF_3$ and the experimentally derived crossover exponent ϕ confirm the theoretical predictions in Refs. 1, 8, and 10.

ACKNOWLEDGMENTS

We wish to thank A. Linz and A. Platzker for providing the samples, R. D. Yacovitch for programming, V. Diorio for technical assistance, and C. C. Becerra for useful discussions. This work was supported by the NSF.

*On leave from the University of São Paulo, S. Paulo, Brazil.

[1]M. E. Fisher, AIP Conf. Proc. 24, 273 (1975). See also, M. F. Fisher and D. R. Nelson, Phys. Rev. Lett. 32, 1350 (1974); M. E. Fisher, *ibid.* 34, 1634 (1975).

[2]A. Aharony, Physica (Utr.) 86-88B, 545 (1977).

[3]W. P. Wolf, Physica (Utr.) 86-88B, 550 (1977).

[4]Y. Shapira and C. C. Becerra, Phys. Lett. A 57, 483 (1976); 58, 493(E) (1976).

[5]Y. Shapira and C. C. Becerra, Phys. Lett. A 59, 75 (1976); Phys. Rev. B 16, 4920 (1977). In Eqs. (6) and (7) of the latter reference, H^2 should be replaced by $H_\perp^2$.

[6]R. D. Yacovitch and Y. Shapira, Physica (Utr.) 86-88B, 1126 (1977).

[7]H. Rohrer and Ch. Gerber, Phys. Rev. Lett. 38, 909 (1977).

[8]J. M. Kosterlitz, D. R. Nelson, and M. E. Fisher, Phys. Rev. B 13, 412 (1976).

[9]C. Domb and A. R. Miedema, in *Progress in Low Temperature Physics*, edited by C. J. Gorter (North-Holland, Amsterdam, 1964), Vol. IV, p. 296ff; H. E. Stanley, J. Appl. Phys. 40, 1272 (1969); D. Jasnow and M. Wortis, Phys. Rev. 176, 739 (1968).

[10]P. Pfeuty, M. E. Fisher, and D. Jasnow, AIP Conf. Proc. 10, 817 (1973); P. Pfeuty, D. Jasnow, and M. E. Fisher, Phys. Rev. B 10, 2088 (1974).

[11]For a summary and references see L. J. de Jongh and A. R. Miedema, Adv. Phys. 23, 1 (1974).

[12]P. H. Cole and W. J. Ince, Phys. Rev. 150, 377 (1966); A. Platzker, Ph.D. thesis (MIT, 1970) (unpublished).

[13]Y. Shapira and C. C. Becerra, Phys. Rev. Lett. 38, 358 (1977); 38, 733(E) (1977).

[14]Y. Shapira and N. F. Oliveira, Jr., Proceedings of the Twenty-third Conference on Magnetism and Magnetic Materials 1977 (to be published).

[15]L. J. de Jongh and D. J. Breed, Solid State Commun. 15, 1061 (1974).

[16]Keystone Carbon Co., St. Marys, Pa.; Model No. L0904-125-H-T2.

[17]H. H. Sample and L. G. Rubin, Cryogenics (to be published). The temperature change due to the H-induced change in the hydrostatic head can be orders of magnitude larger than the H-induced change in the boiling point at a constant pressure.

[18]T. J. Moran and B. Lüthi, Phys. Rev. B 4, 122 (1971).

[19]A. Bachellerie and Ch. Frenois, J. Phys. (Paris) 35, 437 (1974).

[20]R. L. Melcher and D. I. Bolef, Phys. Rev. 178, 864 (1969); 184, 556 (1969); 186, 491 (1969).

[21]Y. Shapira and S. Foner, Phys. Rev. B 1, 3083 (1970).

[22]C. G. Windsor and R. W. H. Stevenson, Proc. Phys. Soc. Lond. 87, 501 (1966).

[23]Several mean-field expressions for the slope $[dT_c^{\parallel}/d(H^2)]$ are given in Ref. 21. One is in terms of J, another in terms of T_n and still another is in terms of the susceptibility χ_N at T_N and T_N itself. Because the mean-field relations between J, T_N, and χ_N are not accurately obeyed in nature, the substitution of experimental values for J, T_N, and χ_N into the three mean-field expressions for the slope leads to different values. These, in turn, lead to three estimates for b: 3.9×10^{-11}, 5.6×10^{-11}, and 2.3×10^{-11} K/Oe^2, respectively. The experimental value $b=4\times10^{-11}$ K/Oe^2 is in reasonable agreement with any of these values. In the text we chose to use the mean-field expression for the slope in terms of J, which we felt was the most fundamental.

[24]P. R. Bevington, *Data Reduction and Error Analysis for the Physical Sciences* (McGraw-Hill, New York, 1969).